Research Article

Photocatalytic and antibacterial activities of AgNPs from Mesua Ferrea seed

N. Thirumagal[1] · **A. Pricilla Jeyakumari**[1]

Received: 21 July 2020 / Accepted: 7 October 2020 / Published online: 24 November 2020

Abstract
The silver nanoparticles have been successfully prepared with *Mesua ferrea* seed extract by biological method. Characterizations have been made by XRD, FTIR, UV–Vis-NIR, FESEM with EDAX, DLS and HRTEM. Crystal structure and dislocation density were characterized by X-ray diffractometer and reveal that synthesized AgNPs were FCC structure and the size of AgNPs were 15 nm. Field Emission Scanning Electron Microscopy (FESEM) and High-Resolution Transmission Electron Microscope (HRTEM) characterizations were used to determine the morphology and size of the Ag nanoparticles in the range of 18–30 nm. The functional groups of AgNPs were identifying by FT-IR analysis. The UV–Vis-NIR spectral analysis is used to study optical behaviors like absorption and transmission properties of the AgNPs and optical bandgap of 2.7 eV. The dynamic light scattering (DLS) results confirm a good stabilization of the Ag nanoparticles. The photocatalytic activity of nanoparticles prepared via the biological method exhibited a higher photocatalytic activity compared to powders obtained by the hydrothermal method. The photocatalytic studies were evaluated for AgNPs by the degradation of Congo red under sunlight irradiation. The synthesized silver nanoparticles were tested against gram + Ve (*Staphylococcus aureus* and *Bacillus subtilis*) and gram − Ve (*Salmonella typhi*) bacteria for different concentrations like (10, 20, 30, and 40 µg/mL) and the results were discussed. The antimicrobial activity of AgNPs displayed a better zone of inhibition against selected human pathogens. The present study also investigated the toxicity effect of biogenic AgNPs against human lung adenocarcinoma cancer cells and normal human epithelial cells in vitro, and the inhibitory concentrations were found to be 30 and 40 µg/mL, respectively. We are anticipated a medicinal plant for the biological synthesis of AgNPs with the effective biomedical applications.

Keywords Silver nanoparticles · *Mesua ferrea* · XRD · Morphology · Antibacterial activity

1 Introduction

In recent times nanoscience and nanotechnology have led to a technological revolution in the world, which is apprehensive with materials with significantly novel and enhanced physical, chemical and biological properties. In this regard, nanoparticles are recognized as antibacterial agents due to their size, structure, and surface properties [1, 2].

Nanomaterials has been widely used in many applications such as transparent conductive films, efficient photocatalysts, varistors, gas sensors, photonics, ceramics, healthcare, cosmetics, food and feed, environmental issue, biomedical application, chemical companies, electronics, drug delivery, energy, optoelectronics, catalysis, single-electron transistors, light emitters, non-linear optical devices and photo-electrochemical applications [3–12]. It has been shown that the size, morphology, stability and properties (chemical and physical) of these nanoparticles

✉ A. Pricilla Jeyakumari, pricilla1510@gmail.com | [1]Department of Physics, Thiruvalluvar Government Arts College, Rasipuram, Tamilnadu, India.

much depend on the preparation technique and conditions they used in the experiment [13–17]. The sol–gel has several advantages such as high purity, ultra- homogeneity, lowering the synthesis temperature and most significantly the possibility of making new compositions [18–29] electrical and optical devices [30–34]. Metallic nanoparticles used in pharmaceutical applications such as anti-cancer, anti-parasite, antimicrobial, antiviral activity [35–39]. Multidrug resistant (MDR) bacteria are well-recognized to be one of the most important current public health problems. Some MDR bacteria have become quite prevalent causes of community-acquired infections. The spread of MDR bacteria into the community is a crucial development, and is associated with increased morbidity, mortality, healthcare costs and antibiotic use. Factors associated with community dissemination of MDR bacteria overlap but are distinct from those associated with nosocomial spread [40–42]. Recently nanostructured AgNPs have engrossed nice attention owing to their in-depth exploitation in environmental and antibacterial drug activity. The antibacterial agents are used to prevent or kill the growth of bacteria. Ag nanoparticles are good antibacterial drug agents. Chemical constituents present in *Garcinia mangostana* tannin, a -mangostin, b -mangostin, g -mangostin,somangostin, gartanin, and 8-desoxygartanina a -mangostin, g -mangostin, gartanin, 8-deoxygartanin, 5,9-dihydroxy-2, 2-dimethyl-8-methoxy-7-(3-methylbut-2-enyl)-2 *H*, 6 *H* –pyrano [3, 2-b] xanthen-6-one, garcinone E, 2-(g, g -dimethylallyl)-1,7-dihydroxy-3-methoxyxanthone, and epicatechin. *Nepheliumlappaceum* L. contains fatty acids in seed lipids are arachidic acid, oleic acid, stearic acid, and palmitic acid, protein, fat, and carbohydrates, aminoaid [43, 44]. The excellent antibacterial drug activity of Ag nanoparticles was probed by several researchers [45–48]. In the modern era, the water is getting depleted by number of pollutants present in the waste effluents from the industries. It is necessary to remove these pollutants from the waste water on the account of their toxicity. The nitro group containing pollutants are of major concern as they are difficult to reduce because of their toxic behavior. But there is a growing demand forfast, effective and improved method for degradation and removal of these hazardous organic dyes.

In recent times, metallic nanoparticles are found to have impressive photocatalytic property for degradation of organic compounds under visible light irradiation [49–53]. Congo red is the sodium salt of benzidinediazo-bis-1-napthyllamine-4-sulfonic acid; It is a diazole dye that is red in alkaline solution and blue in acid solution and used especially as an indicator. Congo red (CR) can also cause allergic dermatitis and skin irritation. Some of them have been reported to be carcinogenic and mutagenic. Karthik et al. describe the photocatalytic properties of SnO_2 prepared by green synthesis [54].

Musea ferrea belongs to guttiferae family and is blessed with a variety of medicinal properties and it is a rich source of secondary metabolites. In Asian countries and are traditionally used by the local people for the treatment of various ailments including asthma, cough, dyspepsia, fever, itchiness, nausea and renal diseases. Several pharmacological attributes of Mesua species such as antioxidant, antimicrobial, antiviral, antitumor and immunomodulatory have already been proved (Teh et al. 2012; Asif et al. 2016). The Chemical constituents present in *Musea ferrea* are α-copaene, germacrene D,ve β-amyrin, mesuanic acid, triterpenoids, resins, tannins, biflavonoids, phenolmesuone.

This paper deals with the synthesis of silver nanoparticles, in the presence of Mesua *ferrea* seed extract of deploying a biological technique, enabling controlled production of shape-modulated high purity nanoparticles. AgNPs were characterized by X-ray diffraction (XRD), Fourier-transform infrared spectroscopy (FTIR), UV–Vis-NIR spectrophotometry, energy-dispersive X-ray spectroscopy (EDX), DLS and field-emission scanning electron microscopy (FESEM). Both particle types were evaluated for their potential use as a photocatalyst, antibacterial activity.

2 Materials and method

2.1 Materials collected

Silver nitrate (99.9%) was purchased from Sigma-Aldrich. The seeds were collected from the Siddha medicals. Double distilled water was used for preparing aqueous solutions all over the experiments.

2.2 Sample preparation

The seeds were collected from the Siddha medical and washed many times in tap water and dry for 3 days in the sunlight and grind to make a powder. 5 g of powder was taken in a beaker and 100 mL of double distilled water for 20 min at 100 °C. The seed extract was filtered through Whatman filter paper and collected for further process.

2.3 Synthesis of silver nanoparticles

There are various top down and bottom approaches for synthesis of AgNPs. In our present investigation, AgNPs have been synthesized by green synthesized method. Because this method is cost effective, eco-friendly, it required low temperature [57–64].

50 mL of 5 mM silver nitrate ($AgNO_3$) solution was added to 10 mL of seed extract dropwise with constant stirring at 60 °C and colour changes were observed to faint red to

brown. This indicates the creation of silver nanoparticles. The extract was then centrifuged at 10,000 rpm for 20 min the pellet was washed two times and calcinated at 200 °C in muffle furnace and the collected powder was then used for characterization and to evaluate antibacterial activity.

2.4 Characterization

The structure of synthesized AgNPs was investigated using the XPERT-PRO X-ray Diffractometer with CuKα$_1$ radiation (1.5406Å). The morphologies were observed by HRTEM (JEOL/JEM 2100F), FESEM (SIGMA HV – Carl Zeiss with Bruker Quantax 200 Z 10 EDS Detector) and equipped with EDS to find the element composition. FT-IR analysis was carried out by JASCO 460 PLUS FT-IR spectrometer in the range of 4000–400 cm^{-1}. Biosynthesized AgNPs were analyzed by using UV–Vis-NIR spectrum (Perkin Elmer Lambda 35). Antibacterial activity of synthesized AgNPs has experimented with *Staphylococcus aureus, Bacillus subtilis,* and *Salmonella typhi,* bacterium by agar disc diffusion technique.

The photocatalytic activity of AgNPs was determined by studying the photodegradation of Congo red dye solution under sunlight irradiation. 20 mg of AgNPs was added to 100 mg/L CR aqueous solution and stirred for 30 min and the mixture was kept under for sunlight for 1–3 h the residual CR in the aqueous solution was analyzed by checking the absorbance at 550 nm. The samples were collected at regular intervals (for every 30 min) and the UV–Vis spectrum was recorded. The degradation percentage of the dye in the presence and absence of AgNPs is calculated from the following equation [65].

$$\eta = \frac{C_0 - C_1}{C_0} x100\% \quad (1)$$

η is the percentage of degradation, C_o is the initial concentration of the dye (mg/L) and C_1 is the concentration of the dye after irradiation in the selected time interval (mg/L).

3 Results and discussion

3.1 Structural analysis

The synthesized AgNPs were crushed as a fine powder for X-ray diffraction studies. The recorded X-ray diffraction pattern for AgPNs is depicted in Fig. 1. The recorded spectrum of the sample was taken at room temperature in a 2θ range of 0–80° using CuKα$_1$ radiation of wavelength 1.54056 Å. From the diffraction pattern, the d-spacing and hkl values for each diffraction peak in the corresponding spectrum of the sample were identified. Using the face center cubic structure crystallographic equation, the lattice parameter values of AgNPs were calculated and compared with the reported

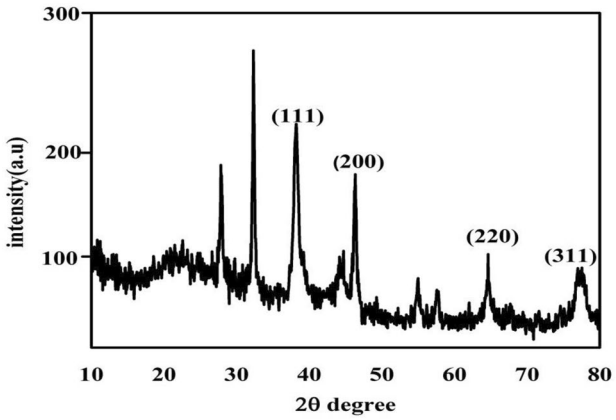

Fig. 1 XRD pattern of AgNPs

values from JCPDS No. 04–0783. It is confirmed that AgNPs belong to the face center cubic crystal system: the unit cell parameters were found to be a = 4.0715 nm. Some additional peaks were reported the presence of bioorganic matters and the capping for AgNPs for the formation [66].

The size of the silver nanoparticles is calculated from the XRD data using Scherrer's formula:

$$D = \frac{k\lambda}{\beta \cos\theta} \quad (2)$$

The average particle size of the Silver nanoparticles is 15 nm.

Willamson-Hall method is used to find the lattice strain by the modified Scherrer equation

$$\frac{dy}{dx}\beta \cos\theta = (k\lambda/D) + (4\varepsilon \sin\theta) \quad (3)$$

The W–H plot of βcosθ versus sinθ is shown in Fig. 2. The W–H plot is expected to be a horizontal line parallel to the sinθ axis, whereas in the presence of strain, it has a non-zero slope. The obtained value of microstrain for the silver nanoparticles is 0.00672.

3.1.1 Dislocation density (δ)

The dislocation density (δ) is calculated using the equation.

$$\delta = \frac{1}{D^2} \quad (4)$$

The number of unit cells (n) is estimated from.

$$n = \frac{D^3}{6V} \quad (5)$$

where V is the volume of the unit cell

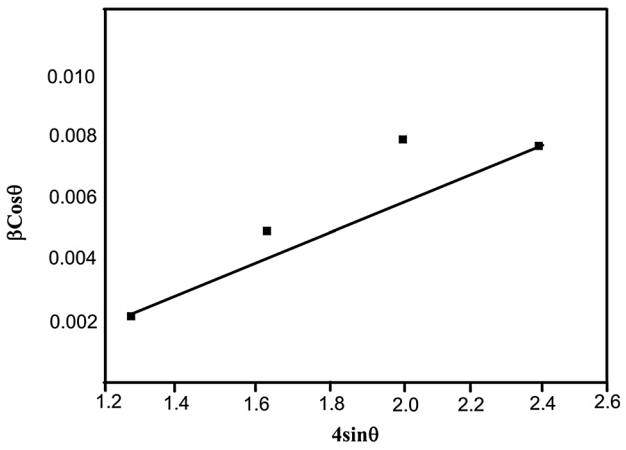

Fig. 2 W–H plot of AgNPs

3.1.2 Morphology index

The Morphology Index (MI) is evaluated from FWHM of XRD. MI is obtained using the equation

$$MI = FWHM_h/FWHM_h + FWHM_p \quad (6)$$

where $FWHM_h$ is the highest FWHM value obtained from peaks and $FWHM_p$ is value of particular peak's FWHM. The calculated MI values are shown in Table 1.

3.1.3 Relative percentage

The Relative Percentage Error (RPE) is calculated by

$$RPE = \frac{Z_H - Z}{Z} X100 \quad (7)$$

where Z_H is the experimental d-values in the XRD pattern and Z is the standard d-values in JCPDS data. The calculated RPE values are presented in Table 1.

3.2 FTIR analysis

The FTIR spectrum was measured with in the 400–4000 cm^{-1} region using JASCO 460 PLUS FTIR spectrophotometer KBr pellet technique. The FTIR spectrum of AgNPs is shown in Fig. 3. The functional groups are present in the AgNPs and *Musea ferrea* seed extract contains alkyl, amines alcohols, phenols in the frequency of 500 cm^{-1}–4000 cm^{-1}. The synthesized powder has an intense vibrational stretching 3850 cm^{-1}–3443 cm^{-1} (–OH) stretching alcohol. The band at 2360 cm^{-1} identified as C–N stretching (Nitriles), 1633 cm^{-1} has been observed as N–H bend primary amines. The band at 1384 cm^{-1} which rose OH bending Phenol, 1068 cm^{-1} has observed as C–OH stretching alkyl ether 668 cm^{-1}indiates alkynes, primary and secondary amines. This results indicates that carboxyl group, amine and phenols groups are mainly involved in the formation of silver nanoparticles [67]. The comparison of seed extract and AgNPs are shown in Table 2.

3.3 Morphology studies of agnps

The FESEM image of AgNPs is shown in the Fig. 4a, b and Table 3 shows that the EDX of AgNPs. The peak indicates the Ag of the energy interval of 3 keV. The small quantities of additional elements, including Ca, Na, O, Mg, C and Ag were associated with *Mesuea Ferrea* seed extract reducing

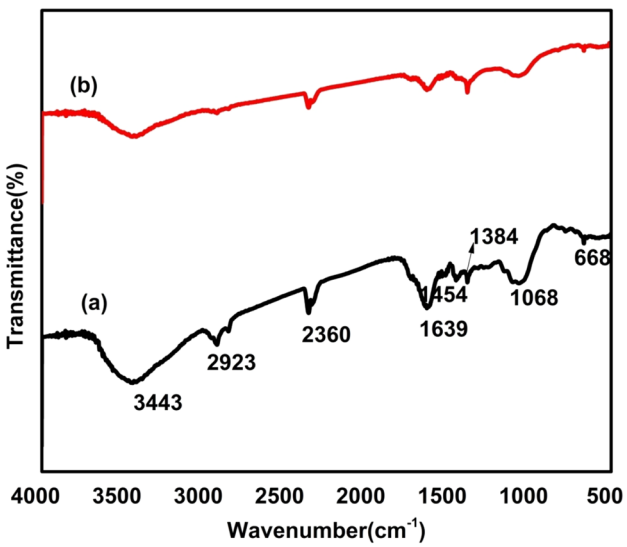

Fig. 3 FTIR spectrums of AgNPs and *Musea ferrea* seed extract

Table 1 Structural properties of FCC silver nanoparticles

2θ°	d-spacing (Å)	Crystalline size D (nm)	Dislocation density (×10^{14} lines/m^2)	Number of unit cells (×10^6)	Morphology index (MI)	Relative percentage error (RPE)
38.25	2.35289	18.1741	3.02	14.78406	0.8856	0.7
44.36	2.04204	10.0605	8.89	2.91814	0.3103	0.1
64.64	1.44176	10.0836	9.83	2.52152	0.9348	0.4
77.64	1.22970	21.5952	2.14	2.47493	0.3913	0.2

Table 2 Comparison of FTIR bands (AgNPs and seed extract)

Vibrational frequencies (cm^{-1})		Assignments
AgNPs synthesized	Seed extract@	Possible functional groups
3443	3443	O–H stretching (Alcohols,Phenols)
2360	2360	C–N stretching (Nitriles)
2923	–	C–H stretching (Alkanes)
1633	1633	N–H bending(Primary amine)
1454	1454	C–H bending(Methyl)
1384	1384	OH stretching(Phenol)
1068	1068	C–O Stretching Alkly ether
668	–	Metals

the silver ions. EDX analysis cannot distinguish between elemental Ag and Ag atoms in other compounds. Fig. 4c shows that the HRTEM images of AgNPs which exhibiting spherical this result is corresponding to the result of coffee Arabica seed extract [68]. Most of the diameter of the particles in the range of 18 nm–30 nm for 5 mM sample. SAED patterns show a strong presence of bright spots along with their crystal orientations appearing within the diffraction rings. The bright spot in the SAED pattern for Fig. 6c the crystalline nature and spots in the form of circle designate the polycrystalline nature. SAED that corresponded to the different crystallographic planes of FCC structure of elemental silver are seen in the Fig. 4c. The XRD spectrum of silver nanoparticles (Fig. 1) exhibiting the

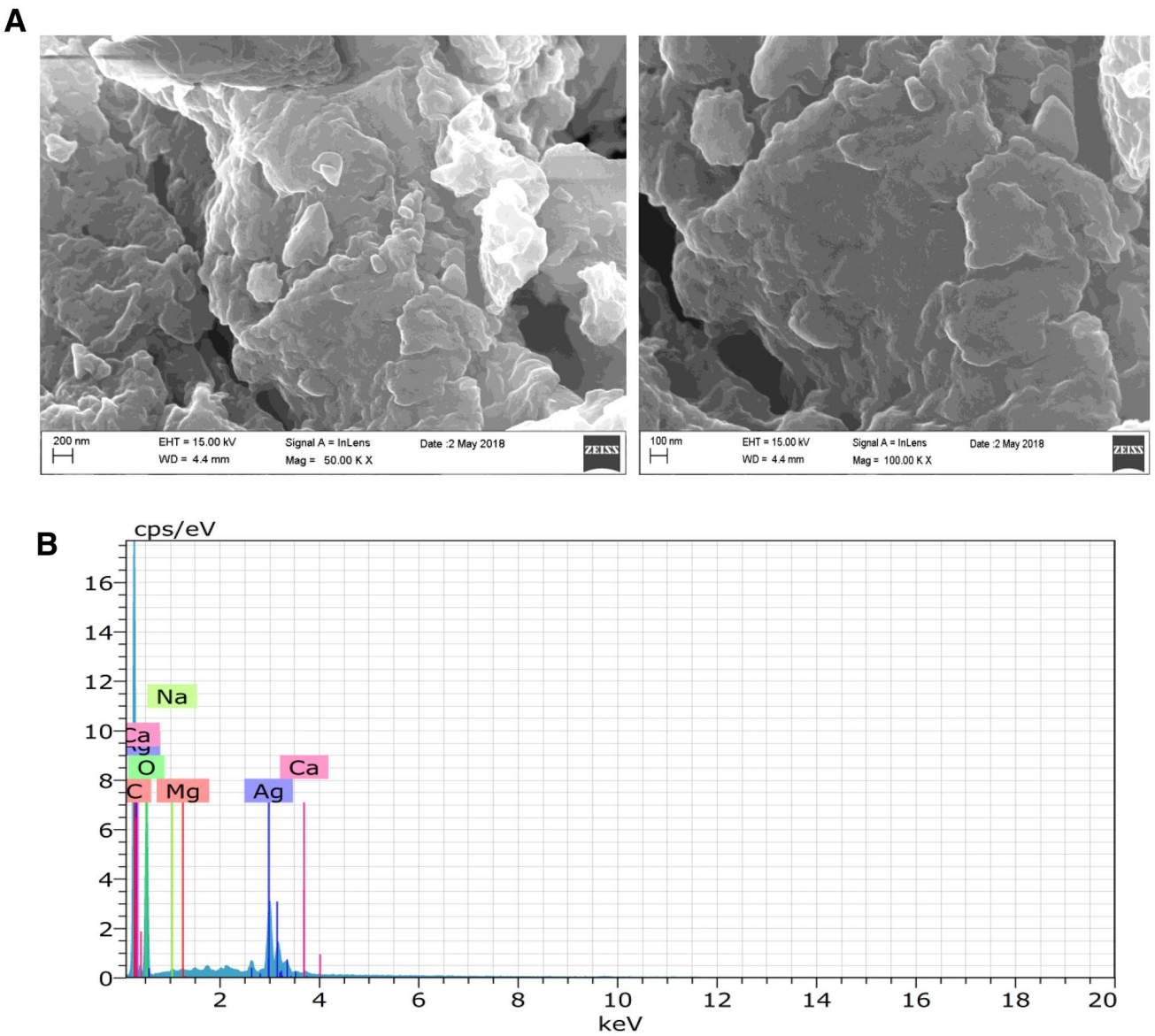

Fig. 4 **a** FESEM images of AgNPs, **b** EDX of AgNPs, **c** HRTEM and Particle size distribution

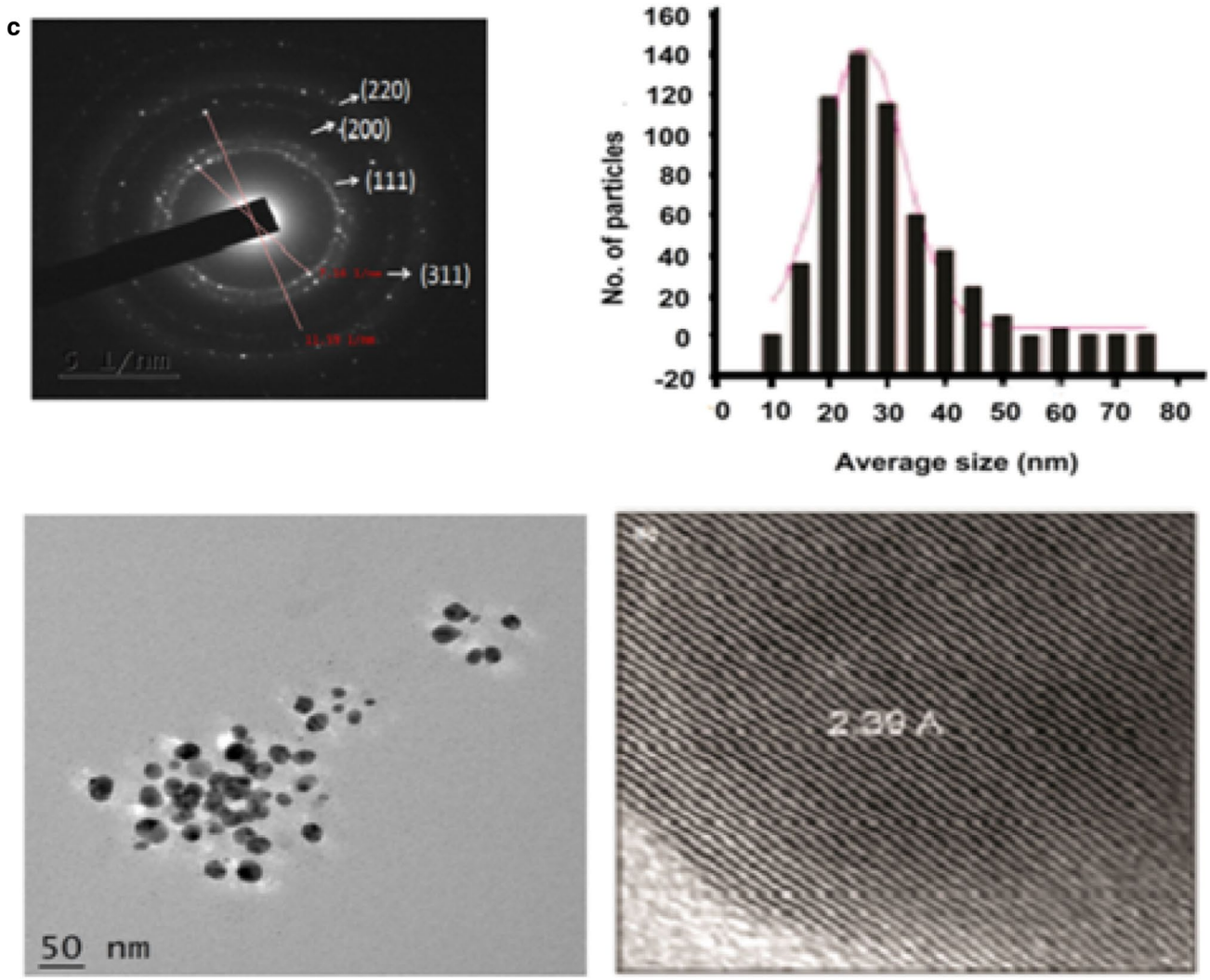

Fig. 4 (continued)

Table 3 EDX analysis of composition from synthesized

Mesuea ferrea AgNPS		
Elements	Weight (%)	Atomic (%)
O	41.31	39.58
Ag	12.40	1.76
Ca	0.39	0.15
Na	0.11	0.08
Mg	0.00	0.00
Total	100.00	100.00

characteristic peaks of the silver nanoparicles observed at 2θ values 38°, 44°, 64°, 77° corresponding to (111), (200), (220), (311)of silver nanoparticles is also agreed with SAED result.

The average number of atoms per nanoparticle by using the formula given below

$$N = \left[\Pi pD^3\right)/(6M)\Big]^* N_A$$
$$N = \left[\left(\Pi\left(1.05x10^{-20}\right)(11)^3\right)/(6(108))\right]^* 6.022x10^{23} \quad (8)$$
$$= 4.078 \times 10^4 \text{atoms/NP}$$

3.4 DLS analysis

The DLS pattern of AgNPs is shown in Fig. 5. The particle distribution was carried out using a DLS instrument. The analysis determines average particles size distribution profile of synthesized nanoparticles. In this result AgNPs were polydispersed in nature with the increased diameter

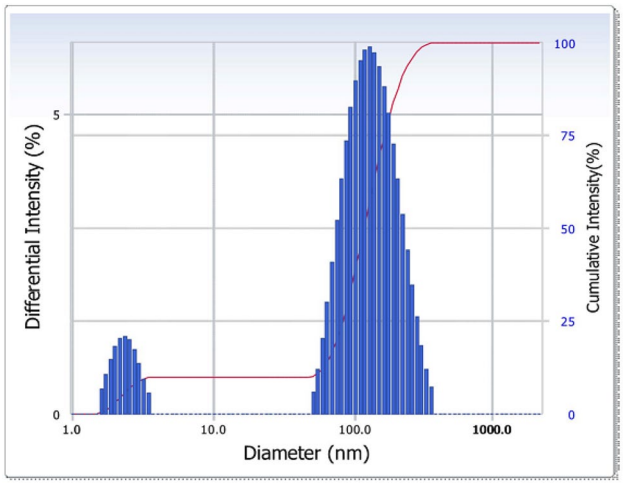

Fig. 5 DLS pattern of synthesized AgNPs using *Mesua ferrea* seed extract

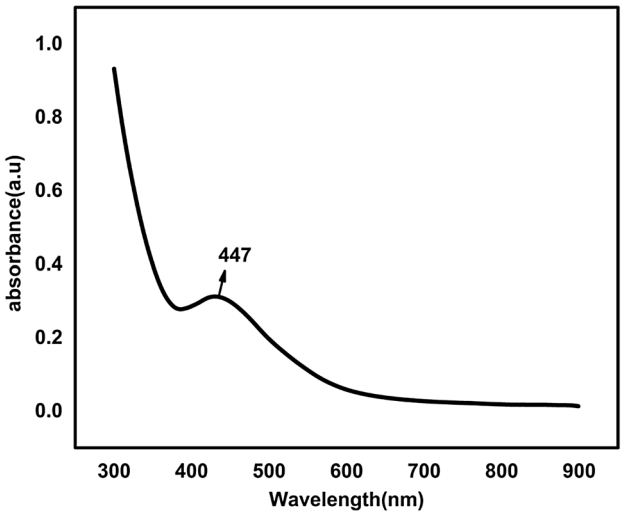

Fig. 6 Optical absorption Spectrum of AgNPs

of particles in the range of 2.4 nm–100 nm. The larger size particles appeared due the agglomeration AgNPs in the solution.

3.5 Optical studies of AgNPs

The spectrum was recorded in the wavelength region 190 nm–1100 nm using the Perkin Elmer Lambda 35 spectrophotometer. The recorded optical absorption spectrum of AgNPs is shown in Fig. 6. The absorption spectrum of the silver colloid in the range of 300 nm–900 nm. UV–visible spectrum was absorbed due to the surface plasma resonance; it is due to the formation of silver colloids because AgNPs exhibit an intense absorption peak at 447 nm. As a direct optical band gap is material, the nanoparticles under study as an optical absorption coefficient (α) obeying the following relation for high photon energies hv.

$$\alpha = \frac{A\sqrt{(h\nu - E_g)}}{h\nu} \tag{9}$$

where E_g is optical band gap of the crystal and A is a constant.

The graph between $(\alpha h\nu)^2$ versus (hv) as shown in Fig. 7. The optical energy band gap (E_g) is estimated as 2.7 eV by extrapolating the linear portion of the graph to meet the energy axis to determine the energy band gap.

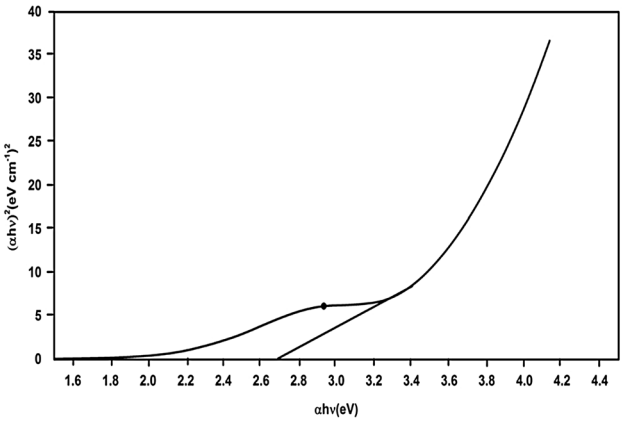

Fig. 7 Optical bandgap of AgNPs

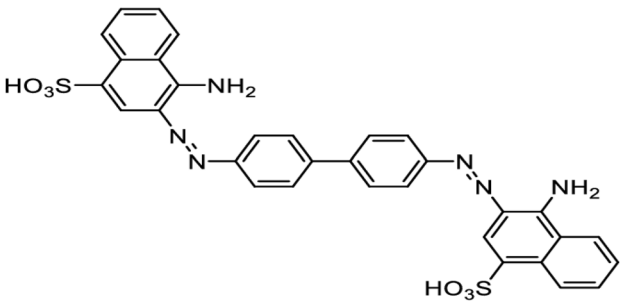

Fig. 8 Molecular structure of Congo red

3.6 Photo catalytic activity

Figure 9 shows the photodecolourisation of Congo red in the presence and absence of AgNPs photocatalyst under sunlight irradiation. There was no observable colour loss of the dye in the absence of catalyst. Slight decolourisation with the photocatalyst in the absence of light may be due to the adsorption of the dye onto AgNPs Complete decolourisation in the presence of light coupled with photocatalyst clearly indicates that the degradation phenomenon

Table 4 Comparison of photoatalytic activity of AgNPs against congo red

Sample	Degradation efficiency (%)	References
AgNPs(Phaseolus vulgaris fruit)	50	69
AgNPS(*Brassica oleracea capitata* fruit)	50–60	70
AgNPs(*Mesua Ferrea* seed)	92	Present work

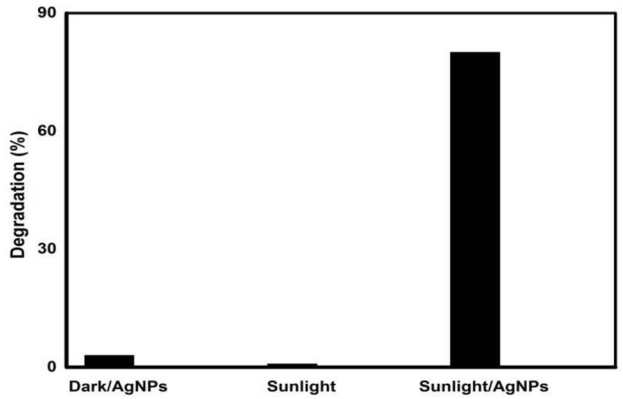

Fig. 9 Presence and absence of catalysts (AgNPs)

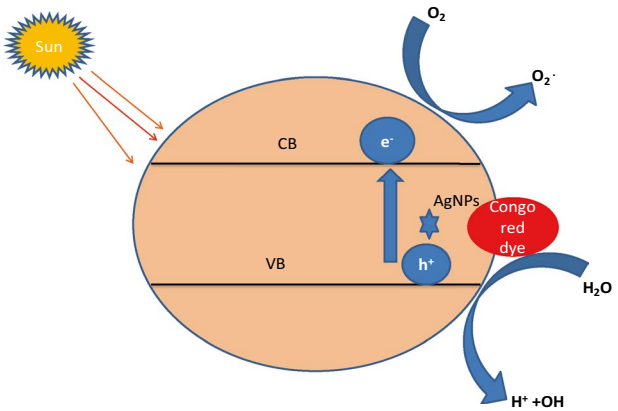

Fig. 10 Schematic diagram of mechanism of photodegradation of Congo red mixed AgNPs

is purely photocatalytic in nature. Molecular formula of Congo red is $C_{32}H_{22}N_6Na_2O_6S_2$ (Fig. 8). The present photocatalytic degradation efficiency is compared with some herbals of AgNPs against Congo red dye (Table 4) and (Fig. 9).

The mechanisms of photocatalytic degradation of Congo red under sunlight as shown in the Fig. 10. Metal nanoparticles support electron transfer from the donor to the acceptor, absorbed photons to excite the valance band electrons to conductions band, due to the

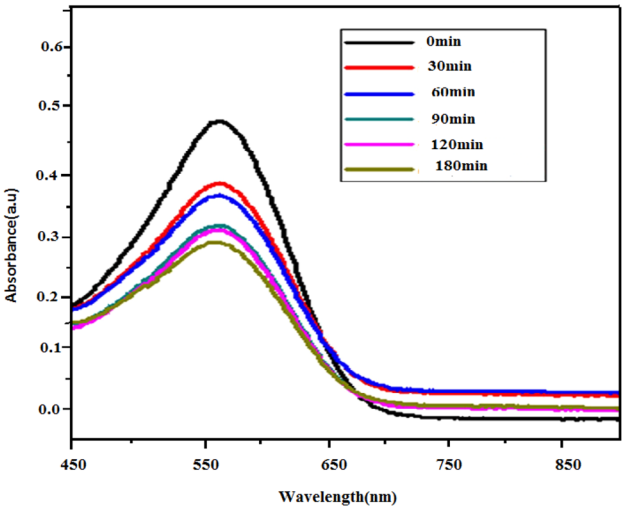

Fig. 11 The Photo catalytic activity of AgNPs

reduction of disintegration the dye molecules conduction band electrons and valance band holes ends. On the other hand during the process when the sunlight is absorbed and ROS (O_2, OH^-, H_2O_2) radicals are formed and cleaning its surfaces by itself. The photocatalytic activity of AgNPs was determined by deoxidation of CR under the natural energy resources sunlight for 2 h–2.30 h Initially, the degradation in the presence of AgNPs has absorbed visually the intensity of the colour gradually decreased with time increased, colour changes dark orange to light the intensity peak absorbed at 550 nm (Fig. 11). Thus Fig. 10 shows that the effective catalytic degradation of AgNPs in the presence of sunlight is faster.

3.7 Photocatalytic mechanism

The electrons in the conductions band react with the dissolved oxygen to form a superoxide anion radical. At the same time, the holes in the valance band react with the adsorbed water to produced hydroxyl radicals. Finally, the superoxide and hydroxyl radicals interact directly with

Table 5 Antibacterial activity of AgNPs using *Mesua ferrea* seed extract concentration (10, 20, 30, 40 µg/mL)

Tested bacteria	Zone of inhibition (mm)			
	10 µg/mL	20 µg/mL	30 µg/mL	40 µg /mL
Staphylococcus aureus	–	9	10	12
Bacillus subtilis	20	22	24	26
Salmonella typhi	10	10	10	10

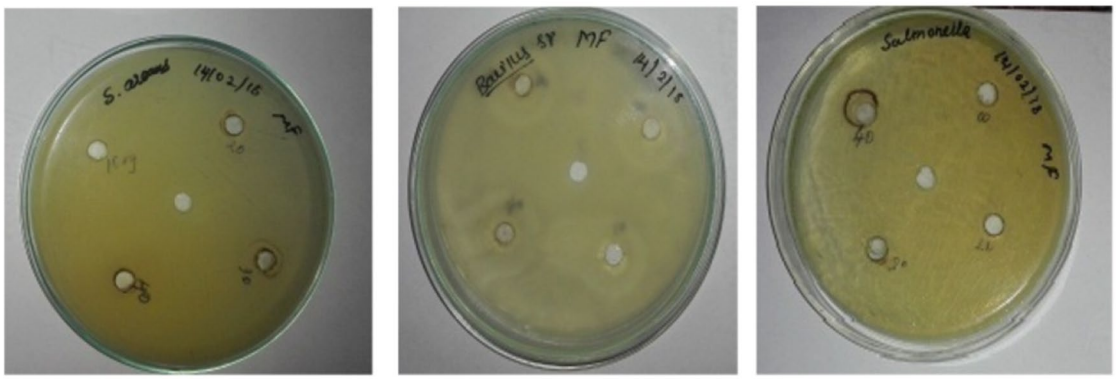

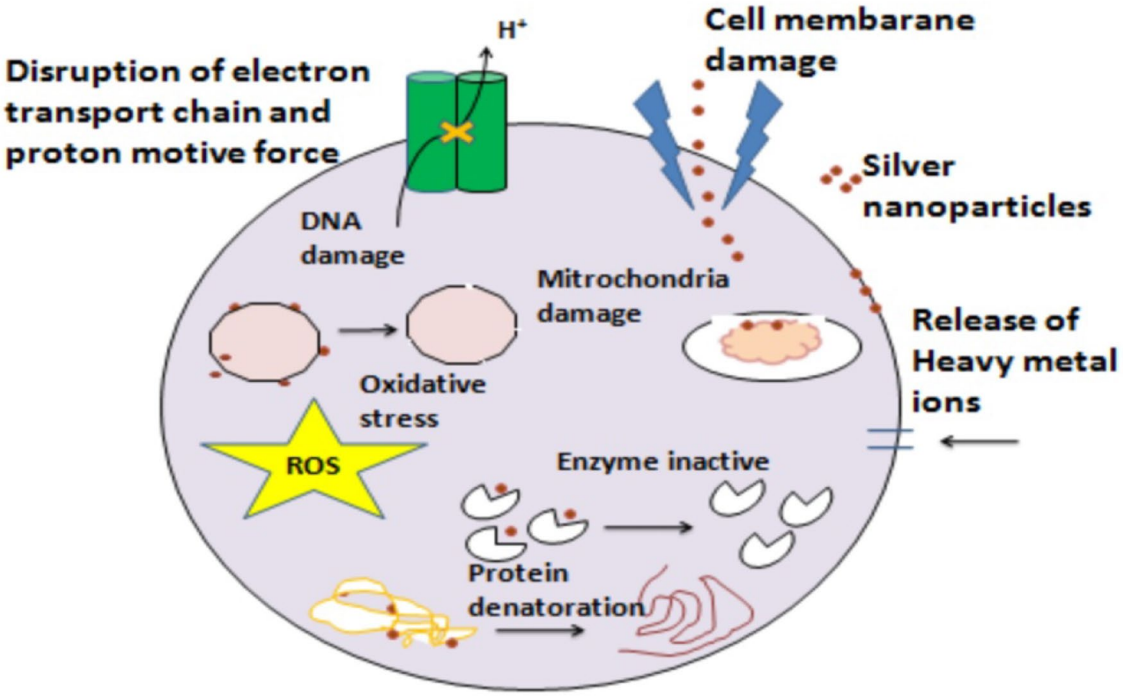

Fig. 12 Mechanism of antibacterial activity

Congo red dye and degrade it into H_2O [71].The photocatalytic mechanisms as follows.

$AgNPs\ (e^-_{CB}) + O_2 \rightarrow AgNPs + O_2.$

$H_2O \rightarrow H^+ + OH.$

$O_2 + H^- \rightarrow HO_2.$

$Silver\ nanoparticles\ (e_{CB}) + HO_2 + H^+ \rightarrow H_2O_2.$

$AgNPs\ (h^+_{vB}) + dye \rightarrow degradation\ products.$

$HO^- + H^+ \rightarrow H_2O_2.$

$HO_2 + e^- \rightarrow HO_2^-$

This result indicates that the silver nanoparticles possess high photo degradation efficiency. The combination of metal nanoparticles generates more active catalytic centres which facilitate the photodegradation performance.

3.8 Antibacterial activity

The antibacterial activity of AgNPs using *Mesua ferrea* seed extract for different concentrations was carried out by the biological method. The zone of inhibition of bacteria is greater than 26 mm as shown in Table 5. This table shows AgNPs have good antibacterial activity against the tested bacteria. The antibacterial activity depends on the size, specific surface area, morphology,

Table 6 Comparison of antibacterial activity for selected human pathogens

Tested	Sample	Zone of inhibition (mm)	References
Staphylococcus aureus	AgNPs + Orange peel	13	[76]
Salmonella typhi	AgNPs + Orange peel	10	[76]
Staphylococcus aureus	AgNPs + Saraca indica	15	[77]
Staphylococcus aure	AgNPs + *Mesua ferrea*	12	Present work
Bacillus subtilis	AgNPs + *Mesua ferrea*	26	Present work
Salmonella typhi	AgNPs + *Mesua ferrea*	10	Present work

etc., the mechanisms of the antibacterial activity are shown in Fig. 12. The mechanism is quite complex, the generation of ROS formation of free radicals with the bactericidal action of AgNPs by the release of Ag^+ ions penetrates negative charge on the cell wall, affect the cell membrane and to disrupt the permeability, damage proteins, and the respiratory of the cell which leads to cell death [72–75]. The antibacterial activities of FCC shaped silver nanoparticles have good zone inhibition compare with other herbals as shown in Table 6.

4 Conclusions

The silver nanoparticles were successfully synthesized using the plant extract of *Mesua ferrea* with high surface area by biological method. XRD results confirmed that the raise in calcinations time resulted in enhance in particle size with a high surface area. The FTIR spectra illustrated the transformation of silver. UV–Vis-NIR absorption spectra revealed that the raise in calcinations time created a blue shift in the spectra, which led to decrease in energy gap with increase in particle size. Based on results, it is concluded that particle size and optical properties are controlled by calcinations time. The morphology and chemical composition were elucidated by FESEM and EDAX. The particle distribution was carried out using DLS studies. In this study, the photocatalytic and antibacterial activity of silver nanoparticles was excellent size 15 nm. It is also concluded that the antimicrobial property of silver nanoparticles increased with increase in surface area to volume ratio due to a decrease in particle size. Hence, smaller sized silver nanoparticles can be used as an antimicrobial agent more effectively. The present study also confirms the antioxidant activity of biosynthesized silver nanoparticles, which can be effectively used as the drug to eradicate free radicals to prevent cellular injury. Due to their high antimicrobial activity, the silver nanoparticles can also be used in the antimicrobial applications. The present study also dealt with the anticancer potential of AgNPs against human lung adenocarcinoma cancer cell line (A549) and normal human epithelial cells (HBL-100), and further study on silver nanoparticles will be carried out for drug delivery, food and pharmaceutical applications.

Compliance with ethical standards

Conflict of interest The author(s) declare that they have no conflict of interests

References

1. Zhen-Xing T, Bin-Feng Lv (2014) MgO nanoparticles as antibacterial agent: preparation and activity. Braz J Chem Eng 31(03):591–601
2. Feyman R (1991) There is plenty of room at the bottom. Science 254:1300–1301
3. Mallikarjuna K, Dillip GR, Narasimha G, John Sushma N, B. Deva Prasad Raju, (2012) Phytofabrication and characterization of silver nanoparticles from piper betle broth. Res J Nanosci Nanotech 2:17–23
4. Meyers MA, Mishra A, Benson DJ (2006) Mechanical properties of nanocrystalline materials. Prog Mater sci 51(4):427–556
5. Schimd G, Chi LF (1998) Metal clusters and colloids. Adv Mater 10(7):515
6. Daniel MC, D. (2004) Astruc"gold nanoparticles: assembly, supramolecular chemistry, quantum-size-related properties, and applications toward biology, catalysis, and nanotechnology". Chem Rev 104(1):293–346
7. Willert M, Rothe R, Landfaster K, Antonietti M (2001) Synthesis of inorganic and metallic nanoparticles by miniemulsification of molten salts and metals. Chem Mater 13(12):4681–4685
8. Colvin V, Schlamp M, Alivisatos A (1994) Light emitting diodes made from cadmium selenidenanocrystals and a semiconducting polymer. Nature 370:354–357
9. Yanagihara N, Uchida K, Wakabayashi M, Uetake Y, Hara T (1999) Effect of radical initiators on the size and formation of silver nanoclusters in poly (methyl methycrylate). Langmuir 15(9):3038–3041

10. Jeon HJ, Yi SC, Oh SG (2003) Preparation and antibacterial effects of Ag-SiO2 thin films by sol-gel method. Biomaterials 24(27):4921–4928
11. Kotthaus SG, Hang BH, Schafer RH (1997) Study of isotropically conductive bondings filled with aggregates of nano-sited Ag-particles. IEEE Trans Compon Packaging Technol 20:15–20
12. Zhao L, Wang H, Huo K, Cui L, Zhang W, Ni H, Zhang Y, Wu Z, Chu PK (2011) Antibacterial nano-structured titania coating incorporated with silvernanoparticles. Biomaterials 32:5706–5716
13. Klaus-Joerger T, Joerger R, Olsson E, Granqvist CG (2001) Bacteria as workers in the living factory: metal-accumulating bacteria and their potential for materials science. Trends Biotechnol 19(1):15–20
14. Hong KHP, Park JL, Sul IH, Youk JH, Kang TJ (2006) Preparation of antimicrobial poly (vinyl alcohol) nanofibers containing silver nanoparticles. J PolymSci Part B PolymPhys 44:2468–2472
15. Cho KH, Park Cho JE, Osaka T, Park SG (2005) The study of antimicrobial activity and preservative effects of nanosilver ingredient. ElectrochimicaActa 51(5):956–960
16. Duran N, Marcato PD, De Suoza GIH, Alves OL, Esposito E (2007) Antibacterial effect of silver nanoparticles produced by fungal process on textile fabrics and their effluent treatment. J Biomed Nanotechnol 3:203–208
17. Jiang H, Manolache S, Wong ACL, Denes FS (2004) Plasma enhanced deposition of silver nanoparticles onto polymer and metal surfaces for the generation of antimicrobial characteristics'. J Appl PolyrSci 93(3):1411–1422
18. Duran N, Marcato PD, Alves OL, de Souza GIH, Esposito E (2005) Mechanistic aspects of biosynthesis of silver nano particles by several *Fusariumoxyporum* strains. J Nanobiotechnol 3:8–14
19. Becker RO (1999) Silver ions in the treatment of local infections. Met based drugs 6:297–300
20. Klaus T, Joerger R, Olsson E, Olssan E, Granqvist CG (1999) Silver based crystalline nanoparticles, microbially fabricated. Procnatlacad sci 96(24):13611–13614
21. Chou KS, Chen CC (2007) Fabrication and characterization of silver core and porous silica shell nanocomposites particles. Micropor Mesopor Mat 98:208–213
22. El-kheshen AA, EL-Rab SFG (2012) Effect of reducing and protecting agents on size of silver nanoparticles and their antibacterial activity. Der Pharma Chemica 4(1):53–65
23. Guzman MG, Dille J, Godet S (2009) Synthesis of silver nanoparticles by chemical reduction method and their antibacterial activity. Int J Chem Biomolecular Eng 2–3:104–111
24. Epifani M, Giannini C, Tapfer L, Vasanelli L (2000) Sol-Gel synthesis and characterization of Ag and Au nanoparticles in SiO2, TiO2 and ZrO2 thin films. J Am Ceram Soc 83(10):2385–2393
25. Kruis FFH, Rellinghaus B (2000) Sintering and evaporation characteristics of gas-phase synthesis of sizeselected PbS nanoparticles. Mater Sci Eng B 69:329–324
26. Magnusson MDK, Malm J, Bovin J, Samuelson L (1999) Gold nanoparticles: production, reshaping, and thermal charging. J Nanoparticle Res 1:243–251
27. Sastry M, Ahmad AA, Khan MI, Kumar R (2003) Biosynthesis of metal nanoparticles using fungi and actinomycete. Curr Sci 85:162–170
28. Iravani S (2011) Green synthesis of metal nanoparticles using plants. Green Chem 13:2638–2650
29. Korbekandi H, Iravani SS, Abbasi S (2009) Production of nanoparticles using organisms. Crit Rev Biotech 29:279–306
30. Silambarasan S, Abraham J (2012) Biosynthesis of silver nanoparticles using the bacteria Bacillus cereus and their antimicrobial property. Int J pharmacypharm Sci 4:536–540
31. Azam A, Ahmed F, Arshi N, Chaman M, Naqvi AH (2009) One step synthesis and characterization of gold nanoparticles and their antibacterial activities against E. coli (ATCC 25922 strain). Inter J Theo App Sci 12:1–4
32. Pillai SC, Kelly JM, McCormack DE, Ramesh R (2004) Microstructural analysis of resistors prepared from nanosize ZnO. Mater Sci Technol 20:964–968
33. Pillai SC, Kelly JM, McCormack DE, Ramesh R (2006) Effect of step sintering on breakdown voltage of varistors prepared from nano-materials by sol gel route. advances in applied ceramics. Adv Appl Ceram 1053:158–160
34. Georgekutty R, Seery MK, Pillai SC (2008) A highly efficient Ag-ZnO photocatalyst: synthesis, properties, and mechanism. J Phys Chem C 112(35):13563–13570
35. Emmanuel R, Ovais M, Padmavathy S, Shinwari ZK, Prakash P (2017) Antimicrobial efficacy of drug blended biosynthesized colloidal gold nanoparticles from *Justicia glauca* against oral pathogens: a nanoantibiotic approach. Microb Pathog. https://doi.org/10.1016/j.micpath.2017.10.055
36. Saravanan M, Jacob V, Arockiaraj J, Prakash P (2014) Extracellular biosynthesis characterization and antibacterial activity of silver nanoparticles synthesized by bacillus subtilis (NCIM—2266). J Bionanosci. https://doi.org/10.1166/jbns.2014.1201
37. Saravanan Muthupandian, Asmalash Tsehaye, Gebrekidan Atsebaha, Gebreegziabiher Dawit, Araya Tadele, Hilekiros Haftamu, Barabadi Hamed, Ramanathan Kumaresan (2018) Nano-medicine as a newly emerging approach to combat human immunodeficiency virus (HIV). Pharm Nanotechnol. https://doi.org/10.2174/2211738506666180209095710
38. Khatua Ashapurna, Priyadarshini Eepsita, Rajamani Paulraj, Patel Amiyakumar, Kumar Jitender, Naik Aparupa, Saravanan Muthupandian, Barabadi Hamed, Prasad Abhinav, Ghosh Ilora, Paul Bernard, Meena Ramovatar (2020) Potential of emerging gold nanoparticles using *Pongamia pinnata* leave extract: a novel approach in nanoparticle synthesis. J Clust Sci. https://doi.org/10.1007/s10876-019-01624-6
39. Barabadi Hamed, Tajani Babak, Moradi Mona, Kamali Kaveh Damavandi, Meena Ramovatar, Honary Soheila, Mahjoub Mohammad Ali, Saravanan Muthupandian (2019) Penicillium family as emerging nanofactory for biosynthesis of green nanomaterials: a journey into the world of microorganisms. J Clust Sci. https://doi.org/10.1007/s10876-019-01554-3
40. Saravanan Muthupandian, Ramachandran Balajee, Barabadi Hamed (2017) The prevalence and drug resistance pattern of extended spectrum β-lactamases (ESBLs)producing Enterobacteriaceae. Microbial pathog. https://doi.org/10.1016/j.micpath.2017.11.061
41. Saravanan M et al (2020a) A systematic review on drug resistant urinary tract infection among pregnant women in developing countries in Africa and Asia. Infect Drug Resist. https://doi.org/10.2147/IDR.S250654
42. Kahsay Atsebaha Gebrekidan, Muthupandia Saravanan (2016) A review on Sero diversity and antimicrobial resistance patterns of Shigella species in Africa, Asia and South America. BMC res note. https://doi.org/10.1186/s13104-016-2236-7
43. Ragasa Consolacion Y, Tabin Theresa Joyce, Reyes Jo Madeleine Ann, Maria Tan Carmen S, Shen Chien-Chang (2016) Chemical constituents of garcinia mangostana pulp and seeds. International J Pharma Clin Res 8(8):1166–1169
44. Mahmood Kaiser, Kamilah Hanisah, Alias Abd Karim, Ariffin Fazilah (2018) Nutritional and therapeutic potentials of rambutan fruit (*Nephelium lappaceum*L.) and the by-products: a review. J Food Measurement Characterization 12:1556–1571. https://doi.org/10.1007/s11694-018-9771-y
45. Gunalan S, Sivaraj R, Rajendran V (2012) Green synthesized ZnO nanoparticles against bacterial and fungal pathogens. Prog Nat Sci: Mater International 22(6):693

46. Karunakaran C, Rajeswari V, Gomathisankar P (2011) Enhanced-photocatalytic and antibacterial activities of sol–gel synthesized ZnO and Ag-ZnO. Mater Sci Semicond Process 14:133–138
47. Jeeva LV, Sharath R, Chandraprabha MN, Neelufar E, Hazra A, Patra M (2012) Synthesis, characterization and evaluation of antimicrobial activity of zinc oxide nanoparticles. J Biochem Technol 3(5):151
48. Arefi MR, Rezaei-Zarchi S (2012) Synthesis of zinc oxide nanoparticles and their effect on the compressive strength and setting time of self-compacted concrete paste as cementitious composites. Int J Mol Sci 13:4340–4350
49. Rani Pooja, Kumar Vanish, Singh Prit Pal, Matharu Avtar Singh, Kim Ki-Hyun, Singh Jagpreet, Rawat Mohit (2020) Highly stable AgNPs prepared via a novel green approach for catalytic and photocatalytic removal of biological and non-biological pollutants. J Environ International. https://doi.org/10.1016/j.envint.2020.105924
50. Singh Karanveer, Kukkar Deepak, Singh Ravinder, Kukkar Preeti, Singh Jagpreet, Rawat Mohit, Kumar Akshay, Kim Ki-Hyun (2019) In situ green synthesis of Au/Ag nanostructures on a metal-organic framework surface for photocatalytic reduction of p-nitrophenol. J Ind Eng Chem. https://doi.org/10.1016/j.jiec.2019.09.008
51. Kaur N, Mehta A, Mishra A, Chaudhary S, Rawat M, Basu S (2018) Amphiphilic carbon dots derived by cationic surfactant for selective and sensitive detection of metal ions. Mater Sci Eng C. https://doi.org/10.1016/j.msec.2018.10.058
52. Kaur Jasneet, Singh Jagpreet, Rawat Mohit (2019) An efficient and blistering reduction of 4-nitrophenol by green synthesized silver nanoparticles. SN Appl Sci. https://doi.org/10.1007/s42452-019-1088-x
53. Singh et al (2011) Green' synthesis of metals and their oxide nanoparticles: applications for environmental remediation. J Nanobiotechnol. https://doi.org/10.1186/s12951-018-0408-4
54. Karthik K, Revathi V, Tatarchuk Tetiana (2018) Microwave-assisted green synthesis of SnO_2 nanoparticles and their optical and photocatalytic properties. Mol cryst liq cryst 671(1):17–23. https://doi.org/10.1080/15421406.2018.1542080
55. Teh SS, Ee GCL, Mah SH, Lim YM, Rahmani M (2012) Mesua beccariana (Clusiaceae), a source of potential anti-cancer lead compounds in drug discovery. Molecules 17:10791–10800
56. Asif M, Shafaei A, Jafari SF, Mohamed SK, Ezzat MO, Abdul Majid AS, Oon CE, Petersen SH, Kono K, Abdul Majid AMS (2016) Isoledene from *Mesua ferrea*oleo-gum resin induces apoptosis in HCT 116 cells through ROS-mediated modulation of multiple proteins in the apoptotic pathways: a mechanistic study. Tox Lett 257:84–96
57. Saravanan et al (2020b) Emerging antineoplastic biogenic gold nanomaterials for breast cancer therapeutics: a systematic review. International J Nanomed. https://doi.org/10.2147/IJN.S240293
58. Vahidi Hossein, Barabadi Hamed, Saravanan Muthupandian (2020) Emerging selenium nanoparticles to combat cancer: a systematic review. J Clust Sci. https://doi.org/10.1007/s10876-019-01671-z
59. Barabadi Hamed, Vahidi Hossein, Kamali Kaveh Damavandi, Rashedi Masoumeh, Hosseini Omid, Ghomi Ahmad Reza Golnaraghi, Saravanan Muthupandian (2020) Emerging theranostic silver nanomaterials to combat colorectal cancer: a systematic review. J Clust Sci. https://doi.org/10.1007/s10876-019-01668-8
60. Barabadi Hamed, Vahidi Hossein, Kamali Kaveh Damavandi, Hosseini Omid, Mahjoub Mohammad Ali, Rashedi Masoumeh, Shoushtari Fereshteh Jazayeri, Saravanan Muthupandian (2020) Emerging theranostic silver nanomaterials to combat colorectal cancer: a systematic review. J Clust Sci. https://doi.org/10.1007/s10876-019-01650-4
61. Barabadi Hamed, Hosseini Omid, Kamali Kaveh Damavandi, Shoushtari Fereshteh Jazayeri, Rashedi Masoumeh, Haghi-Aminjan Hamed, Saravanan Muthupandian (2019) Emerging theranostic silver nanomaterials to combat lung cancer: a systematic review. J Clust Sci. https://doi.org/10.1007/s10876-019-01639-z
62. Balachandar Ramalingam, Gurumoorthy Paramasivam, Karmegam Natchimuthu, Barabadi Hamed, Subbaiya Ramasamy, Anand Krishnan, Boomi Pandi, Saravanan Muthupandian (2019) Plant-mediated synthesis, characterization and bactericidal potential of emerging silver nanoparticles using stem extract of *phyllanthus pinnatus*: a recent advance in phyto-nanotechnology. J Clust Sci. https://doi.org/10.1007/s10876-019-01591-y
63. Kanagamani Krishnaswamy, Muthukrishnan Pitchaipillai, Shankar Karikalan, Kathiresan Ayyasami, Barabadi Hamed, Saravanan Muthupandian (2019) Antimicrobial, cytotoxicity and photocatalytic degradation of norfloxacin using *kleinia grandiflora* mediated silver nanoparticles. J Clust Sci. https://doi.org/10.1007/s10876-019-01583-y
64. Boom Pandi, Poorani Gurumallesh Prabu, Palanisamy Subramaniyan, Selvam Samayanan, Ramanathan Ganesan, Ravikumar Sundaram, Barabadi Hamed, Prabu Halliah Gurumallesh, Jeyakanthan Jeyaraman, Saravanan Muthupandian (2019) Evaluation of antibacterial and anticancer potential of polyaniline-bimetal nanocomposites synthesized from chemical reduction method. J clust sci. https://doi.org/10.1007/s10876-019-01530-x
65. Sathiya Priya A, Geetha D, Karthik K, Rajamoorthy M (2019) Investigations on the enhanced photocatalytic activity of (Ag La) substituted nickel cobaltite spinels. Solid State Sci. https://doi.org/10.1016/j.solidstatesciences.2019.105992
66. Satishkumar M, Sneha K, Won SW et al (2009) Cinnamon zeylanicum bark extract and powder mediated green synthesis of nano-crystalline silver particles and its bactericidal activity. Coll Surf B 73(2):332–338
67. Arumugam et al (2016) Green synthesis of silver nanoparticles using *Zingiber officinale* extract and evaluation of their antioxidant, antimicrobialand anti-inflammatory. World J Pharm Sci 5(11):1219–1234
68. Dhand V, Soumya L, Bharadwaj S, Chakra S, Bhatt D, Sreedhar B (2016) Green synthesis of silver nanoparticles using Coffea arabica seed extract and its antibacterial activity. Mater Sci Eng C 58:36–43
69. Deb S. Int J Chem Tech Res. 2014; 6:3909–3917
70. Sunkar S, Nachiyar CV, Karunya A et al (2013) Phytogenic silver nanoparticle synthesis with potential antibacterial activity and dye degrading ability. Res J Pharm Biol Chem Sci 4:1088–1097
71. Kannan K et al (2020a) Structural and biological properties with enhanced photocatalyticbehaviour of CdO-MgO nanocomposite by microwave-assisted method. Optik 204:164221. https://doi.org/10.1016/j.ijleo.2020.164221
72. Aswini R, Murugesan S, Kannan Karthik (2020) Bio-engineered TiO_2 nanoparticles using *Ledebouria revoluta*extract: larvicidal, histopathological, antibacterial and anticancer

activity. Int J Env Anal Chem. https://doi.org/10.1080/03067319.2020.1718668
73. Rangayasami Aswini, Kannan Karthik, Joshi Swetha, Subban Murugesan (2020) Bioengineered silver nanoparticles using *Elytraria acaulis*(L.f.) Lindau leaf extract and its biological applications. Biocatalysis and Agricultural Biotechnology 27:101690. https://doi.org/10.1016/j.bcab.2020.101690
74. Kannan K et al (2020b) Facile microwave-assisted synthesis of metal oxide CdO-CuO nanocomposite: photocatalytic and antimicrobial enhancing properties. Optik 218:165112. https://doi.org/10.1016/j.ijleo.2020.165112
75. Kannan K et al (2020c) Nanostructured metal oxides and its hybrids for photocatalytic and biomedical applications. Adv Coll Interface Sci 281:102178
76. Balashanmugam P, Nandhini R, Vijayapriyadharshini V, Kalaichelvan PT. Biosynthesis of silver nanoparticles from orange peel extract and its antibacterial activity against fruit and vegetable pathogens. Int J Inn Res Eng 2347–3207
77. Perugu Shyam, Nagati Veerababu, Bhanoori Manjula (2016) Green synthesis of silver nanoparticles using leaf extract of medicinally potent plant Saraca indica: a novel study. Appl Nanosci. https://doi.org/10.1007/13204-015-0486-7